Supporting Information

A Rigid-flexible Binder for Sulfurized Polyacrylonitrile Cathode for Rechargeable Lithium Battery

Calculation of Bond Energy

Hydrogen bond types and bonding energies were calculated by using Gaussian 16 software package[1] to the DFT method. Geometry optimizations and frequency calculations were carried out at the B3LYP[2]-D3[3] levels of theory with the 6-311G(d,p)[4] basis set. The single point energy was calculated at the same functional with 6-311+G(d,p).

In order to eliminate the influence of Basis Set Superposition Error (BSSE) on the calculation accuracy of the interaction energy, we use the counterpoise correction (CP) method to calculate the energy error caused by the BSSE to obtain more accurate interaction energy:

$$E(\text{interaction}) = E(AB) + E(BSSE) - E(A) - E(B) \quad (1)$$

Here, E(AB) + E(BSSE) is equal to the BSSE-correction composite energy [5].

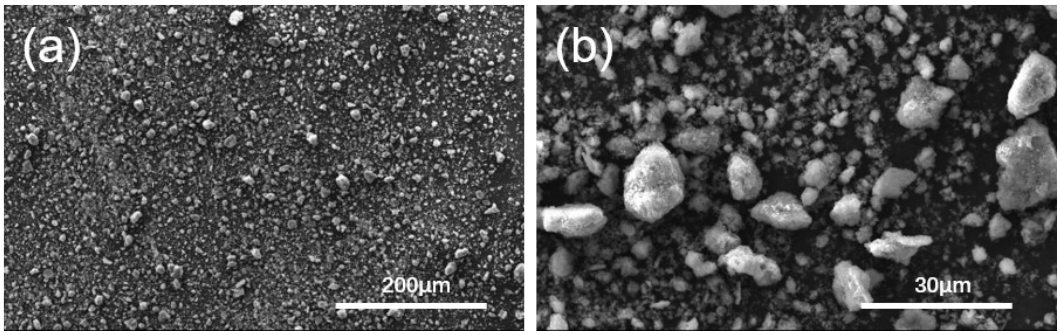

Fig. S1. Micromorphology of Sulfurized Polyacrylonitrile (SPAN).

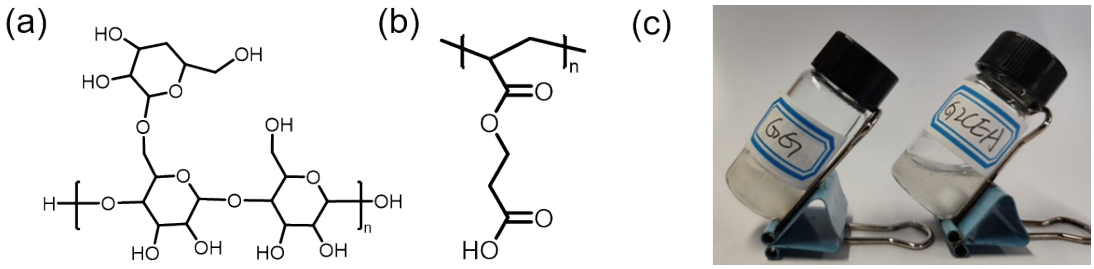

Fig. S2. Structural formula of PCEA (a) and GG (b); (c) Digital photo of GG and G2CEA binder aqueous solution.

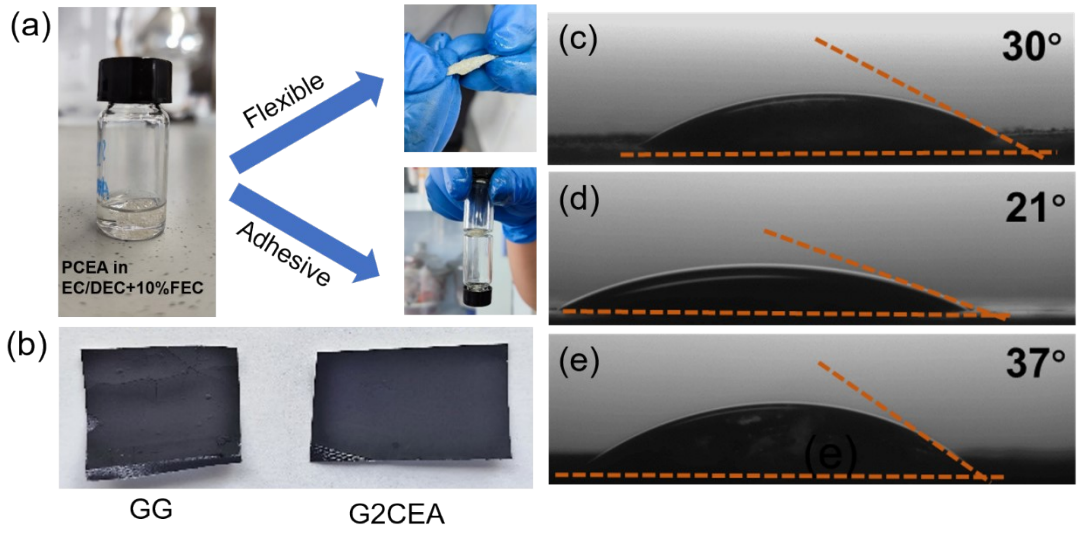

Fig. S3. (a) The state of PECA binder after being soaked in the electrolyte; (b) Digital images of GG and G2CEA-based cathode; (c-e) Contact angles of electrolyte on the GG(c), G2CEA(d), PCEA(e) films;

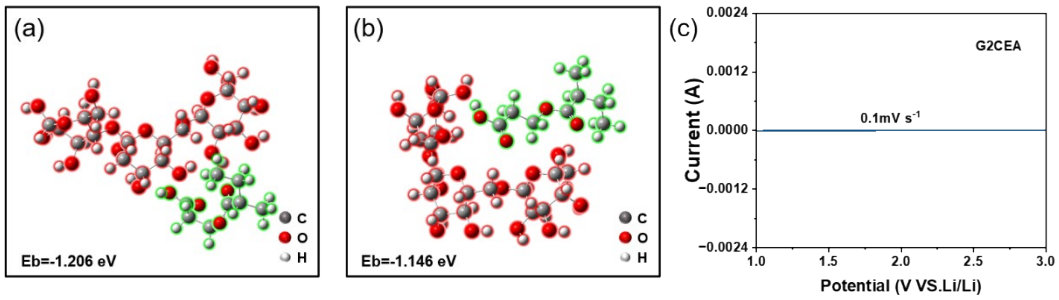

Fig. S4. (a-b) The binding energy between GG and PCEA at different sites; (c) CV curve of Super P/G2CEA(1:1) at scan rate of 0.1 mV s^{-1}.

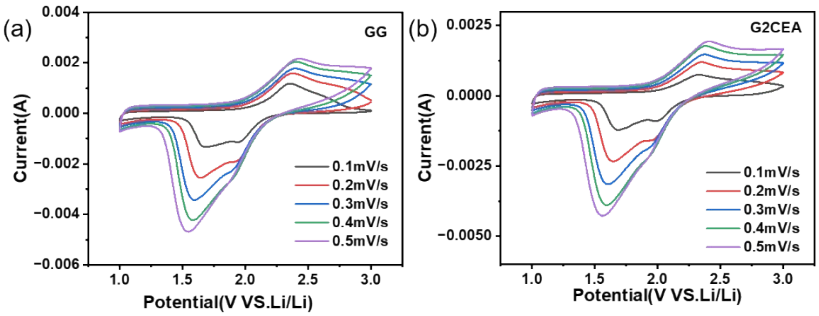

Fig. S5. (a-b) CV curves at increasing scan rates of GG-based (a) and G2CEA-based (b) cells

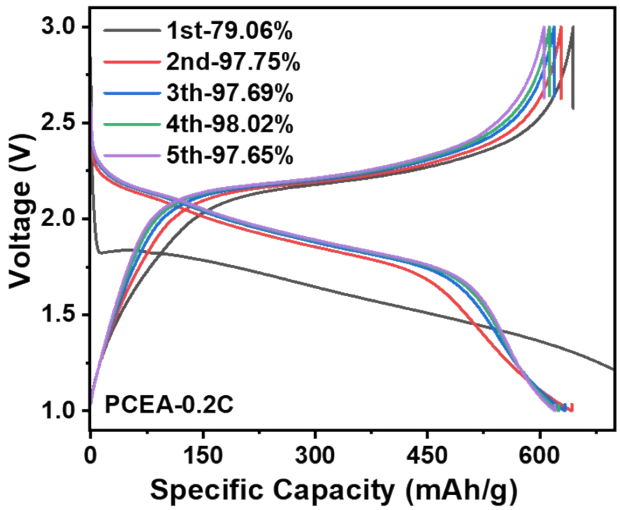

Fig. S6. The charge-discharge curves of the PCEA -based cathode for the first five cycles

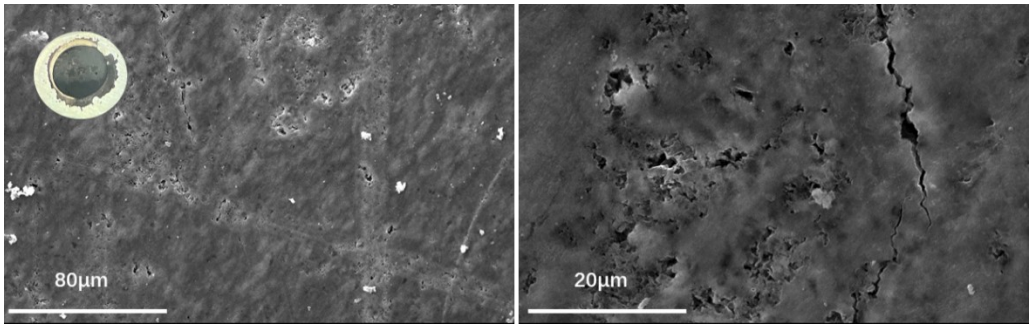

Fig. S7 SEM images of cycled Li anode after 100 cycles at 0.5 C

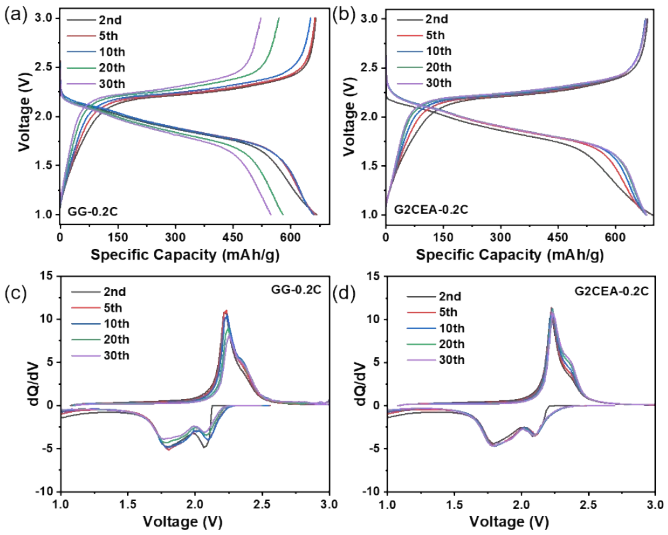

Fig. S8. (a-b) Charge/discharge profiles of GG-based (a) and G2CEA-based (b) cell; (c-d) dQ/dV-Voltage curves of GG-based (c) and G2CEA-based (d) cell.

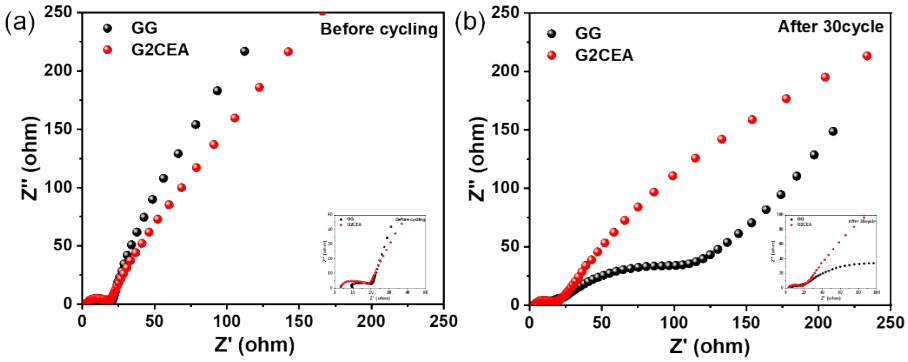

Fig. S9. EIS of GG-based and G2CEA-based cells. (a) Before cycling; (b) After 30 cycles

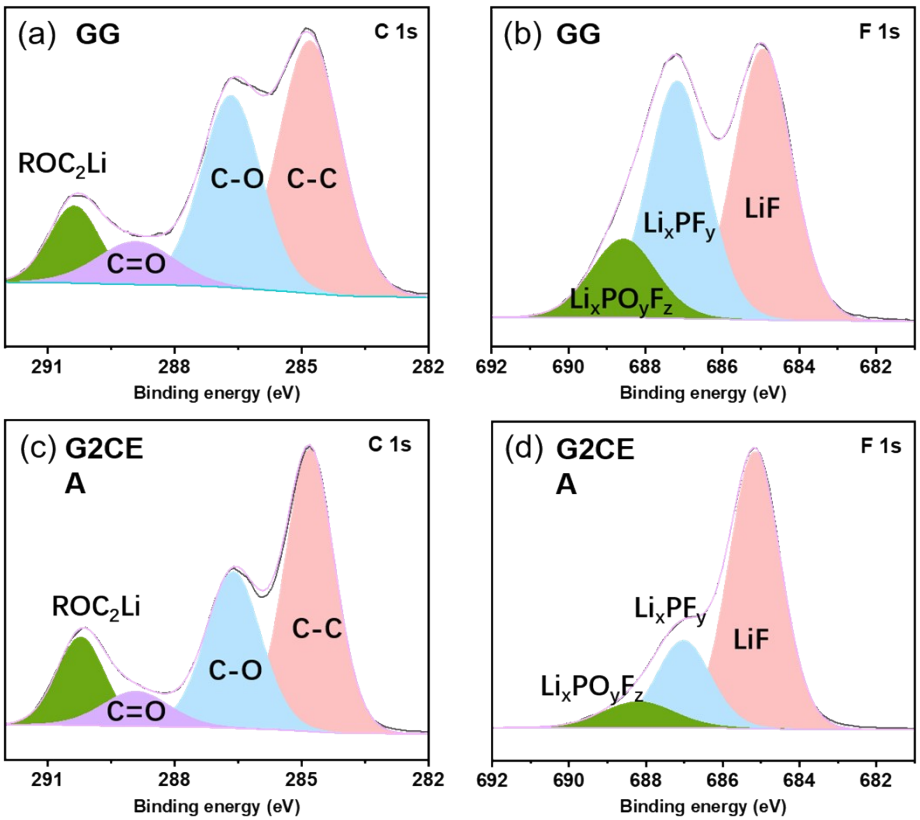

Fig. S10. (a-b) The XPS spectra of SPAN electrode with GG and G2CEA binders. (a) C 1s with GG; (b) F 1s with GG; (c) C 1s with G2CEA; (d) F 1s with G2CEA;

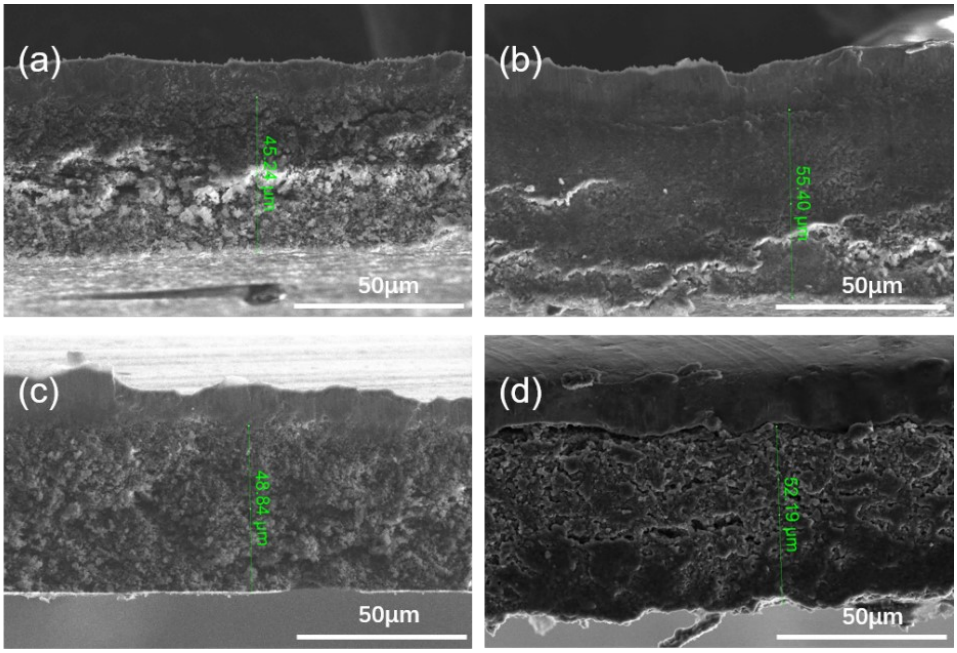

Fig. S11. The cross-sectional SEM images of (a-b) GG and (c-d) G2CEA after 30 cycles.

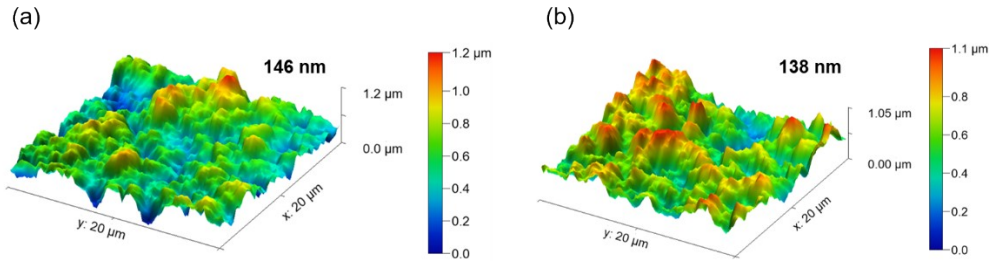

Fig. S12. AFM images of SPAN electrodes before the cycle. (a) GG; (b) G2CEA

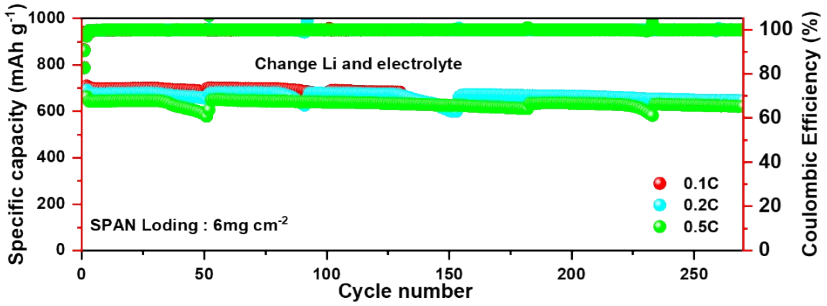

Fig. S13. Long cycle performance of G2CEA based cells at 0.1C, 0.2 and 0.5 C

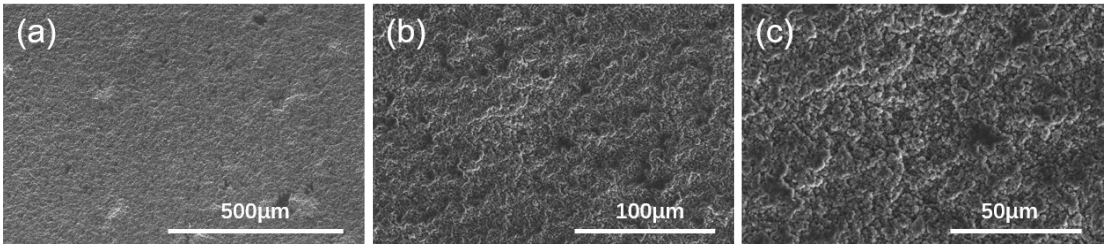

Fig. S14. (a-c) SEM images of G2CEA cathode (6 mg cm^{-2}) at 0.2C after 280cycle

Table S1. Elemental analysis of SPAN composite materials

Element	N %	C %	H %	S %	Theoretical specific capacity mAh g^{-1}
SPAN	13.73	37.39	0.88	46.59	779.0

Table S2. Comparisons of cycling performances of SPAN-based cathodes with different binders.

Binders	Electrode Composition (S: Conductive addition: Binder)	Mass Loading (mg cm^{-2})	Cycle retention

This Work	8 (SPAN): 1: 1	7.5	97.6% after 164 cycles at 0.1C
β-CDp-Cg-2AD[6]	7 (S/C)：1.5：1.5	7.36 mg cm^{-2}	95.8% after 100 cycles at 0.1C
P(AA-co-AM-co-PEGMEA)[7]	8 (FeS_2): 1: 1	7.0 mg cm^{-2}	76.9% after 300 cycles at 0.1C
SA-Co-PEDOT[8]	8 (S/CMK-3): 1: 1	4.3 mg cm^{-2}	76.9% after 100 cycles at 0.1C
PMG-PA-2[9]	6 (S): 3(KB): 1	5 mg cm^{-2}	70.0% after 100 cycles at 0.2C
HMM/PAA[10]	7 (S): 2(KB): 1	4.2 mg cm^{-2}	About 79.0% after 90 cycles at 0.2C
PPTU[11]	7(S/C): 2: 1	5.8 mg cm^{-2}	79.0% after 90 cycles at 0.5C
GB-Y[12]	8 (S/KB): 1: 1	6.56 mg cm^{-2}	About 70.0% after 150 cycles at 0.1C
CWPU[13]	8 (S/C): 1: 1	6.68 mg cm^{-2}	83% after 35cycles at 0.1C

References

[1] Frisch M, Clemente F. MJ Frisch, GW Trucks, HB Schlegel, GE Scuseria, MA Robb, JR Cheeseman, G. Scalmani, V. Barone, B. Mennucci, GA Petersson, H. Nakatsuji, M. Caricato, X. Li, HP Hratchian, AF Izmaylov, J. Bloino and G. Zhe, Gaussian.;9.

[2] Lee C., Yang W., Parr R. G., Phys. Rev. B. 37 (1988) 785-789.

[3] Grimme, S.; Antony, J.; Ehrlich, S.; Krieg, J., J. Chem. Phys. 2010, 132 154104.

[4] Castro E. V. R. Jorge F. E., J. Chem. Phys. 108 (1998) 5225-5229.

[5] K. S. Kim, P. Tarakeshwar, J. Y. Lee, Chem. Rev. 2000, 100, 1445.

[6] T. Zhang, R. Mao, W. Jiang, B. Li, Z. Song, S. Liu, X. Jian, F. Hu. Nano Energy 2023, 114, 108603.

[7] H. Liu, Z. Wu, H. Wang, X. Niu, H. Li, L. Wang. ACS Energy Lett. 2024, 9, 4666.

[8] S. Cui, W. Li, H. Hu, T. Wang, Y. Xing, J. Yin, M. Zhang, W. Liu, S. T. Myung, Y. Jin. Small 2024, 20.

[9] M. Lu, K. Chen, Z. Jia, J. Ren, P. He, S. Yang, R. Bagherzadeh, F. Lai, Y. Miao, T. Liu. Energy Storage Mater. 2024, 73, 103870.

[10] S. Liang, J. Zhang, C. Jia, Z. Luo, L. Zhang. Carbon N Y 2024, 222, 118807.

[11] J. Jian, Q. Chen, H. Sun, R. Li, Y. Hou, Y. Liu, J. Liu, H. Xie, J. Zhu. J. Energy Chem. 2024, 97, 228.

[12] F. Zhou, Y. Mei, Q. Wu, H. Li, J. Xu, H. Chen. Energy Storage Mater. 2024, 67, 103315.

[13] J. Chen, X. Geng, C. Wang, X. Hou, H. Wang, Q. Rong, N. Sun, W. Liu, L. Hu, X. Fu, J. Lei, Z. Liu, X. He. J. Mater. Chem. A Mater 2024, 12, 11038.